

Supplemental Online Content

Mishra N, Ng J, Strom MA, et al. Human polyomavirus 9—an emerging cutaneous and pulmonary pathogen in solid organ transplant recipients. *JAMA Dermatol*. Published online February 9, 2022. doi:10.1001/jamadermatol.2021.5853

eMethods.

eTable 1. qPCR analysis of RNA and DNA extracts

eTable 2. Full genome mutational analyses

eFigure 1. Additional Clinical Photographs

eFigure 2. Skin histopathology and ISH of patients

eFigure 3. Genomic organization of HPyV9

eFigure 4. Control experiments on skin biopsies

eFigure 5. Lung autopsy findings in Patient 3

eReferences

This supplemental material has been provided by the authors to give readers additional information about their work.

eMethods.

Nucleic acid extractions

Total DNA and RNA from frozen tissues were extracted using All prep mini DNA/RNA kit (Qiagen, Hilden, Germany). FFPE tissues were extracted with RecoverAll™ Total Nucleic Acid Isolation Kit for FFPE (Thermo Fisher Scientific). 250- μ l plasma or swabs in viral transport medium were extracted using All Prep DNA/RNA Mini Kit to elute 100 μ l DNA and 50 μ l RNA. DNase treatments to deplete all DNA molecules from RNA samples were performed using TURBO DNA-free kit (Invitrogen AM1907). Nucleic acid concentration and purity were determined on the TapeStation system (Agilent) for subsequent VirCapSeq-VERT and BacCapSeq library preparations and qPCR analysis.

Library preparation and capture sequencing with VirCapSeq-VERT

DNA and RNA extracts of frozen skin biopsies from patient 1 (USD-14), RNA extracts of banked FFPE tissues from patient 2 (USD-16) and patient 3 (USD-19) were subjected to high-throughput sequencing using VirCapSeq-VERT platform (eTable 1).¹ The VirCapSeq-VERT Capture Panel covers the genomes of all viruses known to infect vertebrates (including humans) and enables 100-1000X sensitive detection of viral sequences in complex sample types, compared unbiased Illumina sequencing.

DNA extracts from USD-14 were also used for BacCapSeq to identify bacterial pathogenic agents (eMethods 3).² Individual libraries for each sample were prepped for viral sequencing with the Hyper Prep kit (KAPA Biosystems, Boston, MA, USA) using unique barcodes. Synthesized double-stranded DNA generated from cDNA was sheared to an average fragment size of 200 bp with enzymatic shearing. Sheared products were purified using AxyPrep Mag PCR cleanup beads (Axygen/Corning, Corning, NY), and libraries were constructed using KAPA library preparation kits (Wilmington, MA) with input quantities of 100 to 200 ng DNA. Libraries were purified (AxyPrep), quantitated by Bioanalyzer (Agilent). Libraries were pooled and hybridized with the VirCapSeq-VERT probe sets prior to a final PCR and sequencing on the MiSeq and NextSeq systems¹. The libraries were then mixed with a SeqCap HE universal oligonucleotide, SeqCap HE index oligonucleotides, and COT DNA and vacuum evaporated at 60°C for approximately 40 min. Dried samples were mixed with 2 μ l hybridization buffer and hybridization component A (Roche/NimbleGen) prior to denaturation at 95°C for 10 min. The VirCapSeq-VERT probe library (4.5 μ l) was added and hybridized at 47°C for 12 h in a standard PCR thermocycler. SeqCap Pure capture beads (Roche/ NimbleGen) were washed twice, mixed with the hybridization mix, and kept at 47°C for 45 min with vortexing for 10 s every 10 to 15 min. The streptavidin capture beads complexed with biotinylated VirCapSeq- VERT probes were trapped (DynaMag-2 magnet; Thermo, Fisher) and washed once at 47°C and then twice more at room temperature with wash buffers of increasing stringency. Finally, beads were suspended in 50 μ l water and directly subjected to post hybridization PCR (SeqCap EZ accessory kit V2; Roche/NimbleGen). The PCR products were purified (Agencourt Ampure DNA purification beads; Beckman Coulter, Brea, CA, USA) and quantitated by Tape Station system (Agilent) for Illumina sequencing.

Library preparation and capture sequencing with BacCapSeq

Individual libraries for each sample were prepped for bacterial sequencing also with the Hyper Prep kit (KAPA Biosystems, Boston, MA, USA). Extracted DNA from each sample was sheared to an average fragment size of 200 bp (E210 focused ultra-sonicator; Covaris, Woburn, MA) and remaining steps were same as VirCapSeq-VERT sequencing protocol. DNA libraries were pooled and hybridized with the BacCapsSeq probe sets prior to a final PCR and sequencing on the NextSeq 500 system²

Sequencing and phylogenetic data analysis

After VirCapSeq-VERT and BacCapSeq sequencing, one hundred and fifty base pair single end reads were generated by, which were de-multiplexed using bcl2fastq software v 1.8.4 into individual samples for further analysis. The demultiplexed FastQ files were adaptor trimmed using cutadapt (v 3.0)³. Adaptor trimming was followed by generation of quality reports using FastQC software (v 0.11.5)⁴ which were used to determine filtering criteria based on the average quality scores of the reads, presence of indeterminate nucleotides and homo-polymeric reads. The reads were quality filtered and end-trimmed with PRINSEQ software (v 0.20.3)⁵ and cleaned of human host sequences using Bowtie 2 mapper (v2.2.9)⁶. The host subtracted fastq files were submitted to NCBI SRA database (submission number, SUB8442462). De-novo assembly of quality filtered and host subtracted reads was performed using MIRA Assembler (v4.0). Assembled contiguous sequences (contigs) and unique singletons were subjected to homology search against the entire GenBank nucleotide database using MegaBLAST. The unassigned contigs without any alignments from MegaBLAST were further subjected to protein alignments with NCBI BLASTx. Based on MegaBLAST and BLASTx analysis, the viral and bacterial genomes matching with Illumina reads and contigs were downloaded from NCBI and used for mapping to recover partial or complete genomes and determine genome consensus sequence, depth and breadth of coverage. Reads and contigs matching with HPyV9 were imported to Geneious (V 10.2.6) software. Coding regions of complete genomes were recovered and non-coding control region (NCCR) were recovered by RCA-PCRs (eFigure 3A). Genomes aligned closely with HPyV9 reference sequence (5026 bp long, accession number NC_015150.1).⁷ Genomic organization was similar to HPyV9 reference genome (>99.7% nucleotide similarity and >99.4% aa homology) with same length of open reading frames for VP1, VP2, VP3, small T and large T antigens. VP1 gene based evolutionary and phylogenetic analysis by Maximum Likelihood method was conducted in MEGA X (eFigure 3B).⁸ The phylogenetic analysis revealed clustering of USD14, USD16 and USD19 in same lineage along with HPyV9 reference sequence. VP1 was conserved at nucleotide and protein level in USD-14, USD-16, and USD-19. USD-14, USD-16, and USD-19 had >99.7% nucleotide identity and >99.4% amino acid homology with

HPyV9 reference genome or among each other in VP2, VP3, LT and sT regions. USD-14, USD-16, and USD-19 had five non-synonymous mutations (1 in VP2, 1 in VP3, 2 in LT and 1 in sT) and one synonymous mutation (in LT) in comparison to HPyV9 reference sequence (eTable 2). USD-19 had only one additional non-synonymous mutation in VP2 (T273GàF91L) and 2 additional synonymous mutations (VP2 and VP3). Genomes had variable length of NCCR (502 bp in reference genome, 464 bp for USD-14, 518 bp for USD-16, and 439 bp of USD-19), but four T antigen-binding elements were consistent with reference genome (eFigure 3C). From these genetic data analyses, in-situ hybridization probes targeting VP1 gene were designed, and a specific qPCR assay was developed to diagnose HPyV9, estimate viral load (HPyV9 DNA), and determine viral replication (HPyV9 mRNA transcripts) in other potential clinical samples.

QuantiGene ViewRNA in-situ hybridization on FFPE skin biopsies and autopsy tissues

To detect HPyV9 VP1 mRNA, in situ hybridization was performed using a Thermo Fisher Scientific viewRNA Tissue Assay Core Kit and Blue Module (Life Technologies Corporation, California, U.S.A.). The viewRNA probe set consisted of multiple probes designed to cover 1,116 base pairs of HPyV9-VP1 mRNA sequence. In brief, after deparaffinization, skin, lung, trachea, kidney, liver, colon, small intestine and bone marrow sections were boiled in 1x pre-treatment for 3 min followed by protease treatment for 10 min; most autopsy acquired tissues examined were fixed overnight in formalin, but a subset of lung and skin tissues obtained from further autopsy sampling required protease treatment for 30 min. Sections were subsequently incubated with a viewRNA™ probe at 40°C for 2 h. After washing 3 times in wash buffer, hybridization with PreAmplifier Mix QT (Thermo Fisher Scientific), Amplifier Mix QT (Thermo Fisher Scientific), and Label Probe 1 (HPyV9-VP1) and Label Probe 6 (Human GAPDH) performed according to the manufacturer's instructions. After incubation with FastBlue and FastRed substrate (Thermo Fisher Scientific, California, U.S.A.), the slides were counterstained with Gill's hematoxylin. Patient and control skin biopsy and autopsy tissue formalin fixed paraffin embedded blocks were prepared per standard protocol by the CUIMC Pathology Core laboratories.

Several control experiments to demonstrate specificity of HPyV9 in ISH binding were performed (eFigure 4). There was no binding in lesional tissue biopsies with an N-gene based Middle Eastern Respiratory Syndrome (MERS) Coronavirus control probe. There was no binding of HPyV9 probes to FFPE skin biopsies from: a patient with HPyV7 infection, a patient with erythema multiforme, and perilesional uninvolved and distant uninvolved site in-patient 3. All biopsies were negative for SV-40 T antigen by immunohistochemistry, demonstrating a lack of similarity in T antigen sequences between BK or JC polyoma viruses and HPyV9.

Duplex Quantitative Real-Time PCR

Banked FFPE tissue from skin biopsies of patient 1, ocular and oral swabs, and urine from patient 3, post therapeutic serum collections from patient 3, and autopsy specimens from patient 3 (eTable 1) were tested with a duplex quantitative PCR targeting VP1 of HPyV9 and RNase P human housekeeping gene.^{9,10} DNA and RNA were extracted from all samples. Additionally, RNA extracts were treated with DNase I enzyme to digest HPyV9 DNA traces, so only mRNA transcripts of HPyV9 would be detected. For duplex real-time qPCR assays, 5 µl of extracted nucleic acid was used with; VP1-FWD-primer- CCTGTAAGCTCTCTCCTTA, VP1-REV-primer- CCTGATAAATTCTGACTTCTTC, VP1-HPyV9-Probe- FAM-CTTGTCTCTGGTCTTATGCCTCA-BHQ1, RNase P-FWD-primer-AGATTTGGACCTGCGAGCG, RNase P-REV-primer- GAGCGGCTGTCTCCACAAGT, and RNase P-Probe- CY5 TTCTGACCTGAAGGCTCTGCGCG-BHQ-3 using RNA UltraSense™ One-Step Quantitative RT-PCR System (Thermo Fisher Scientific). The volume was brought up to 25 µl with nuclease-free water (Invitrogen). All real-time qPCR assays were performed using BioRad CFX 96 touch and the following protocol: initial denaturation step at 95 °C for 10 min, followed by 45 cycles of denaturation for 15 s at 95 °C and annealing/extension for 1 min at 60 °C.

Supplemental Autopsy Information

Autopsy Findings

Other notable organ findings include numerous circumscribed tan-brown skin nodules (~0.4 – 1.7 cm in greatest dimension) consistent with previously described keratoacanthomas on upper and lower extremities (eFigure 2), cardiomegaly (530 g) with right and left atrial dilatation and left ventricular hypertrophy, hepatomegaly (1800 g) with sinusoidal dilatation and centrilobular patchy hepatocyte loss, and mild acute diffuse hypoxic-ischemic encephalopathy in the brain. Sample biopsies, serum and autopsy specimens were negative for SARS-CoV-2 RNA.

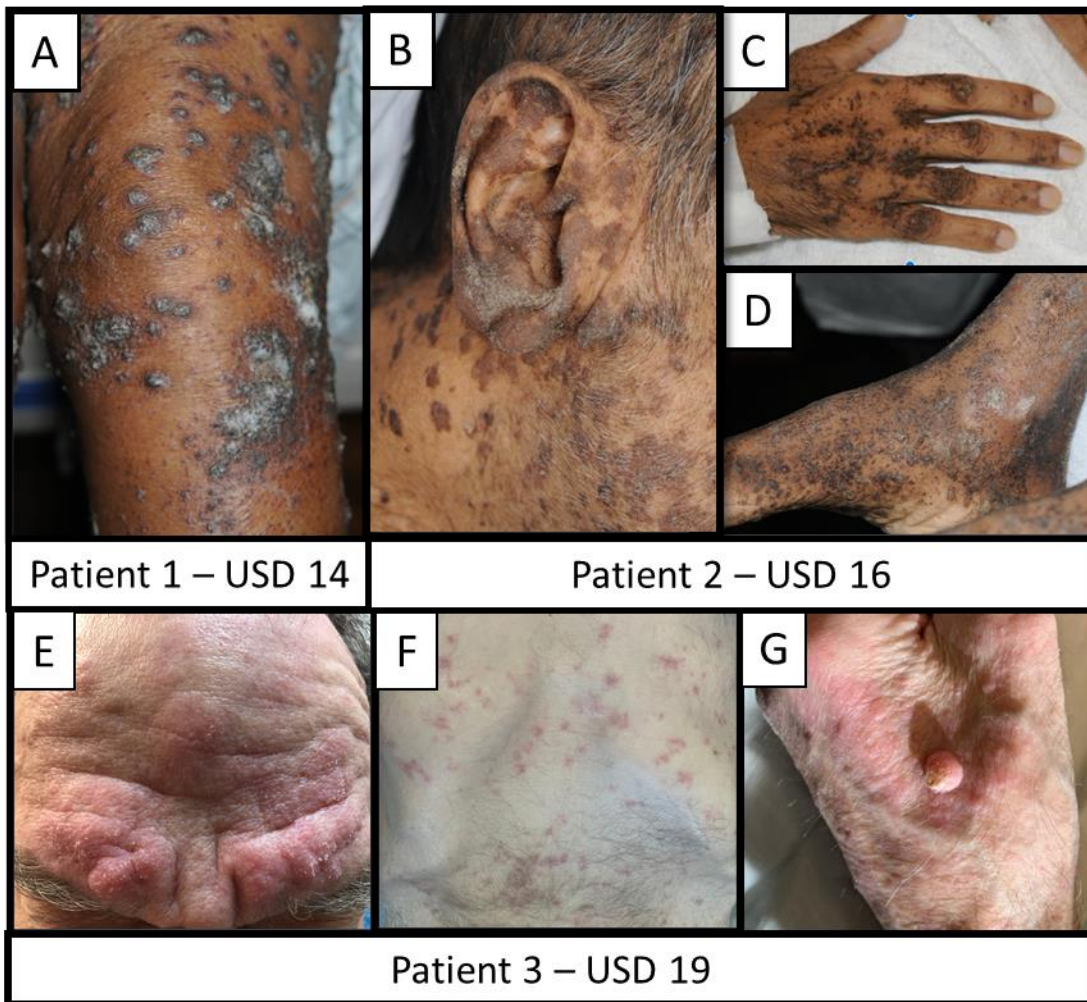
Patient	Sample Type	RNA*/DNA	Viral load (Ct values)	Viral copy number/PCR Reaction	Samples subjected for VirCapSeq-VERT
Patient 1 (USD-14)	Skin lesion biopsy-I	RNA*	13.60	3.68E+06	Yes
	Skin lesion biopsy -II	RNA*	12.20	7.83E+06	Yes
	Skin lesion biopsy -II	RNA*	13.40	3.97E+06	Yes
	Serum	DNA	27.10	1.92E+03	Yes
		RNA*	ND	NA	Yes
	Skin lesion biopsy-FFPE	RNA*	21.50	4.48E+04	Yes
Patient 2 (USD-16)	Skin lesion biopsy-FFPE	RNA*	22.40	2.66E+04	Yes
Patient 3 (USD-19)	Skin lesion biopsy-FFPE-I	RNA*	21.60	4.13E+04	Yes
	Skin lesion biopsy-FFPE-II	RNA*	25.30	5.31E+03	Yes
	Skin lesion biopsy-FFPE-III	DNA	20.70	6.88E+04	Yes
		RNA*	21.50	4.41E+04	Yes
	Perilesional unaffected skin (FFPE-x)	DNA	ND	NA	No
		RNA*	ND	NA	No
	Distant unaffected skin (FFPE-y)	DNA	ND	NA	No
		RNA*	ND	NA	No
	Serum -1 (09/28/2020)	DNA	36.00	1.37E+01	No
		RNA*	ND	NA	No
	Serum -2 (10/07/2020)	DNA	35.70	1.62E+01	No
		RNA*	ND	NA	No
	Serum -3 (10/19/2020)	DNA	28.10	1.12E+03	No
		RNA*	ND	NA	No
	Urine	DNA	27.10	1.95E+03	No
		RNA*	ND	NA	No
	Ocular swab	DNA	29.40	5.41E+02	No
		RNA*	ND	NA	No
	Oral swab	DNA	28.40	9.44E+02	No
		RNA*	ND	NA	No
Patient 3 (USD-19) Autopsy samples	Lung	DNA	17.20	3.91E+05	No
		RNA*	30.40	1.44E+02	No
	Trachea	DNA	32.40	1.72E+02	No
		RNA*	ND	NA	No
	Serum	DNA	25.90	4.88E+03	No
		RNA*	28.60	8.22E+02	No
	Ocular swab	DNA	25.90	4.91E+03	No
		RNA*	27.50	1.75E+02	No
	Oral swab	DNA	23.00	3.33E+03	No
		RNA*	23.30	2.66E+03	No

RNA* is DNase treated RNA, ND- not detected, VirCapSeq-VERT: Capture based vertebrate virus sequencing method, NA- not applicable

eTable 1: qPCR analysis of RNA and DNA extracts

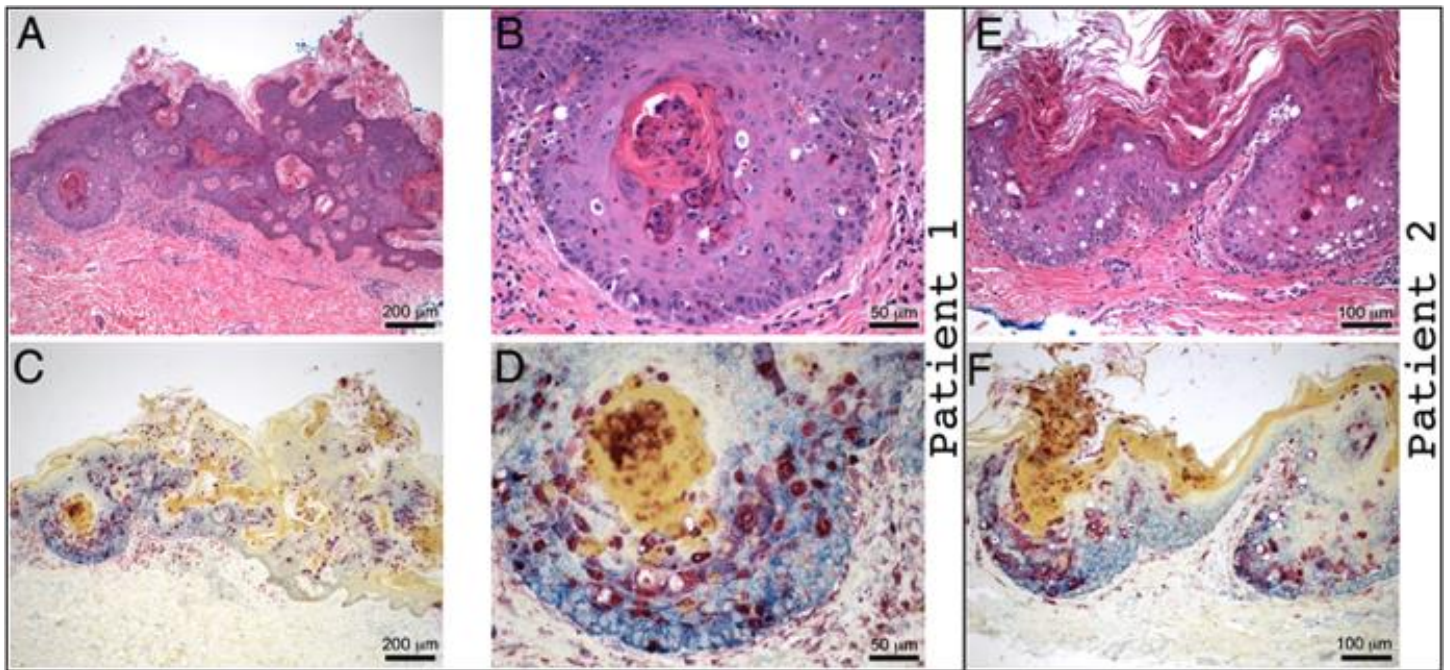
Sample ID	Gene/protein	Gene Length (nt) and location in genome	Protein length (AA)	Human polyomavirus 9, complete genome (NC_015150.1)			
				Nucleotide identity	Amino acid homology	Non-Synonymous mutation	Synonymous mutations
Patient 1 (USD14) (Genome size=4989 bp, accession no. MT416610)	NCCR	464	NA	NA	NA		
	VP1	1116 (1404-2519)	371	100	100		
	VP2	1059 (464-1522)	352	99.9	99.7	C439A (L147I)	
	VP3	702 (821-1522)	233	99.9	99.6	C82A (L28I)	
	LT	2043 (4989-4753/4398-2593)	680	99.9	99.7	G90T (M30I) ; G778A (V260I)	G1797A
	sT	570 (4989-4420)	189	99.8	99.5	G90T (M30I)	
Patient 2 (USD16) (Genome size=5043 bp, accession no. MT416611)	NCCR	518	NA	NA	NA		
	VP1	1116 (1458-2573)	371	100	100		
	VP2	1059 (518-1576)	352	99.9	99.7	C439A (L147I)	
	VP3	702 (702-875)	233	99.9	99.6	C82A (L28I)	
	LT	2043 (5043-4807/4452-2043)	680	99.9	99.7	G90T (M30I) ; G778A (V260I)	G1797A
	sT	570 (5043-4474)	189	99.8	99.5	G90T (M30I)	
Patient 3 (USD19) (Genome size=4964 bp, accession no. MW139299)	NCCR	439	NA	NA	NA		
	VP1	1116 (1387-2502)	371	100	100		
	VP2	1059 (447-1505)	352	99.7	99.4	T273G(F91L), C439A (L147I)	G909A
	VP3	702 (702-1505)	233	99.7	99.6	C82A (L28I)	G552A
	LT	2043 (4964-2568)	680	99.9	99.7	G90T (M30I) ; G778A (V260I)	G1797A
	sT	570 (4964--4395)	189	99.8	99.5	G90T (M30I)	

eTable 2: Full genome mutational analysis



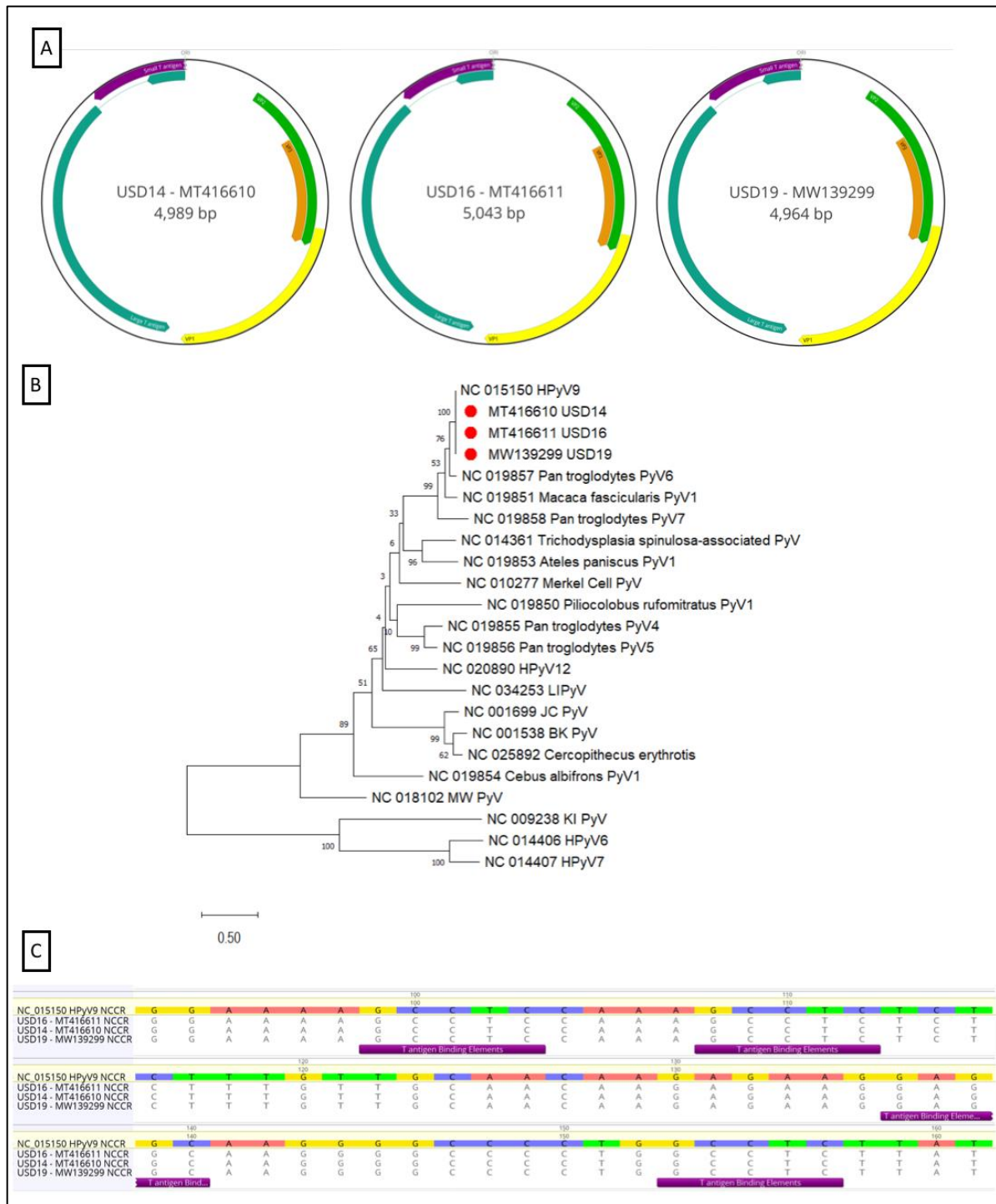
eFigure 1 Clinical Photographs and Histopathology of Patients

Patient 1 (Panel A) is shown several months after initial presentation, with verrucous hyperkeratotic papules and plaques on the lower extremity. Patient 2 (Panels B, C, D) was found to have thin, scaly hyperpigmented papules and plaques on the ears, face, neck and distal extremities, with fewer lesions on the trunk. Patient 3 initially presented with thin pink plaques on the face that subsequently formed plaques with spicules (Panel E). He developed painful keratotic papules and plaques on the distal extremities and trunk (Panels F). As disease progressed, he developed keratoacanthoma-like lesions throughout the body (Panel G).



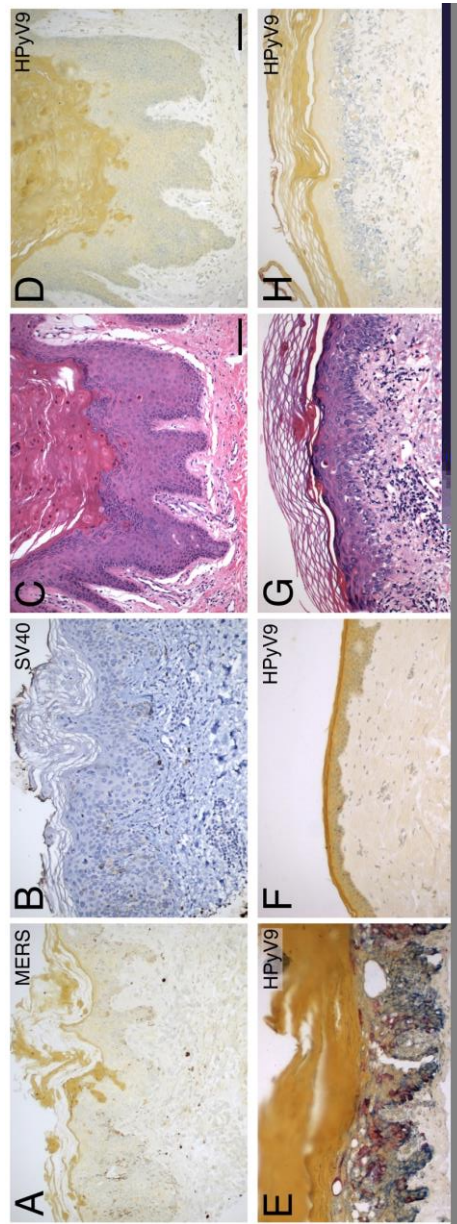
eFigure 2. Skin histopathology of patients.

Hematoxylin & Eosin staining from patient 1 (Panel A and B) and patient 2 (Panel E) demonstrates hyperkeratosis, acanthosis and patchy lymphocytic infiltrates in the superficial dermis, with scattered necrotic, dyskeratotic and vacuolated keratinocytes. *In-situ* hybridization demonstrates human polyomavirus 9 in the cytoplasm and nuclei of keratinocytes (red staining) from patient 1 (Panel C and D) and patient 2 (Panel F). Not displayed here, Periodic acid-Schiff stain, Fite, and Gram stains were negative for infectious agents. In situ hybridization was negative for low and high-risk human papillomavirus. The adnexa were not involved.



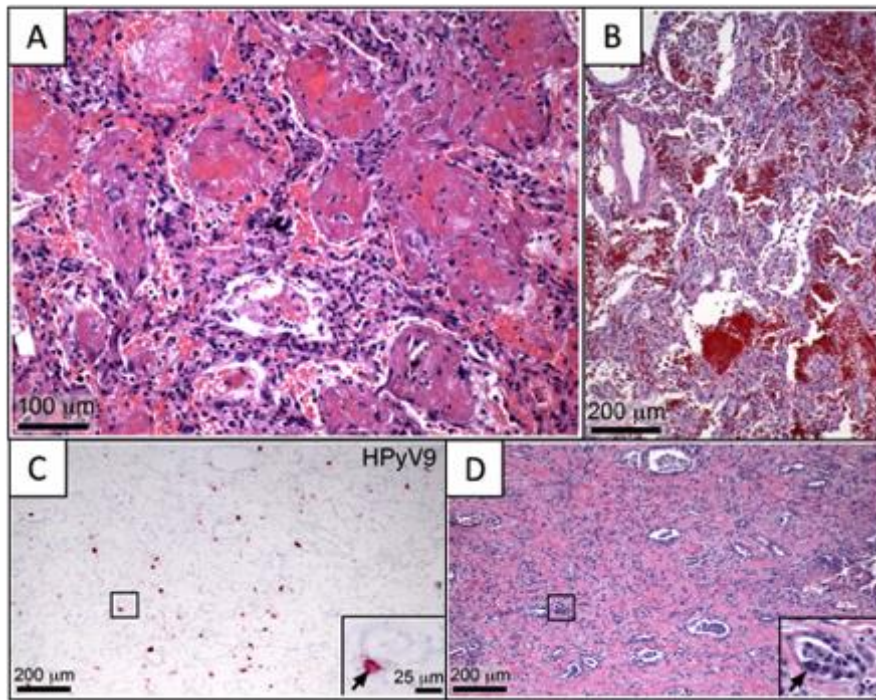
eFigure 3. HPyV9 complete genome organization, phylogenetic analysis

A. Genomic organization of HPyV9 from USD-14, USD-16 and USD-19. **B.** VP1 based phylogenetic tree. The evolutionary history was inferred by using the Maximum Likelihood method and General Reverse Transcriptase model.¹¹ The VP1 tree with the highest log likelihood (-11060.56) is shown. The percentage of trees in which the associated taxa clustered together is shown next to the branches. Initial tree(s) for the heuristic search were obtained automatically by applying Neighbor-Join and BioNJ algorithms to a matrix of pairwise distances estimated using the JTT model, and then selecting the topology with superior log likelihood value. A discrete Gamma distribution was used to model evolutionary rate differences among sites (5 categories (+G, parameter = 0.8916)). The tree is drawn to scale, with branch lengths measured in the number of substitutions per site. This analysis involved 23 amino acid sequences. There were a total of 574 positions in the final dataset. **C.** Demonstration of T antigen-binding elements in NCCR regions of HPyV9 genomes and alignment with HPyV9 reference genome.



eFigure 4. Control experiments on skin biopsies.

Panel A, MERSN *in-situ* hybridization control is negative (lack of red staining) and Panel B, SV40 T antigen immunohistochemistry is negative (lack of brown staining) (Patient 1). Panels C and D, HPyV7 infected skin lesion. Hematoxylin & eosin (H&E) stain (Panel C) demonstrating marked acanthosis, hyperkeratosis and scattered necrotic keratinocytes. There is no hybridization with *in-situ* probe to HPyV9 (Panel D, lack of red staining). Panels E is lesional skin from patient 3 (USD-19). *In-situ* hybridization of HPyV9 demonstrates red staining in the cytoplasm and nuclei of keratinocytes in all layers of the epidermis. Panel F is peri-lesional skin from Patient 3 (USD-19). HPyV9 *in-situ* hybridization is negative (Panel F, lack of red staining). Panels G and H, Control slide of erythema multiforme. H&E stain demonstrating scattered necrotic keratinocytes within the epidermis and a patchy lymphocytic infiltrate (Panel G) and HPyV9 *in-situ* hybridization is negative (Panel H, lack of red staining).



eFigure 5. Lung autopsy findings in Patient 3 (USD-19).

Acute and organizing (Panel A) bilateral diffuse alveolar hemorrhage with hemosiderin laden macrophages and a variably expanded and fibrotic interstitium (Panels A-B, D). HPyV9 (red staining) is present in lung by *in-situ* hybridization (Panels C), seen in macrophages in alveolar space, in alveolar epithelial cells (boxed areas in Panels C, D shown in insets) and in cells scattered in fibrotic interstitium (Panels C). Panels A-B, D: Hematoxylin and eosin stain. Panels C: *In-situ* hybridization for HPyV9.

Supplementary References

1. Briese T, Kapoor A, Mishra N, et al. Virome Capture Sequencing Enables Sensitive Viral Diagnosis and Comprehensive Virome Analysis. *mBio*. 2015;6(5):e01491-01415.
2. Allicock OM, Guo C, Uhlemann AC, et al. BacCapSeq: a Platform for Diagnosis and Characterization of Bacterial Infections. *mBio*. 2018;9(5).
3. Martin M. Cutadapt removes adapter sequences from high-throughput sequencing reads. *2011*. 2011;17(1):3.
4. Andrews S. FastQC: A quality control tool for high throughput sequence data. In. <http://www.bioinformatics.babraham.ac.uk/projects/fastqc.,2010>.
5. Schmieder R, Edwards R. Quality control and preprocessing of metagenomic datasets. *Bioinformatics*. 2011;27(6):863-864.
6. Langmead B, Salzberg SL. Fast gapped-read alignment with Bowtie 2. *Nat Methods*. 2012;9(4):357-359.
7. Scuda N, Hofmann J, Calvignac-Spencer S, et al. A novel human polyomavirus closely related to the african green monkey-derived lymphotropic polyomavirus. *J Virol*. 2011;85(9):4586-4590.
8. Kumar S, Stecher G, Li M, Knyaz C, Tamura K. MEGA X: Molecular Evolutionary Genetics Analysis across Computing Platforms. *Mol Biol Evol*. 2018;35(6):1547-1549.
9. van der Meijden E, Wunderink HF, van der Blij-de Brouwer CS, et al. Human polyomavirus 9 infection in kidney transplant patients. *Emerg Infect Dis*. 2014;20(6):991-999.
10. Mishra N, Ng J, Rakeman JL, et al. One-step pentaplex real-time polymerase chain reaction assay for detection of zika, dengue, chikungunya, West nile viruses and a human housekeeping gene. *J Clin Virol*. 2019;120:44-50.
11. Dimmic MW, Rest JS, Mindell DP, Goldstein RA. rtREV: an amino acid substitution matrix for inference of retrovirus and reverse transcriptase phylogeny. *J Mol Evol*. 2002;55(1):65-73.